

## Neoclassical effects on transport in the helical states of RFX-mod plasmas

M.Gobbin<sup>1</sup>, G.Spizzo<sup>1</sup>, L.Marrelli<sup>1</sup>, D.Terranova<sup>1</sup>, E.Martines<sup>1</sup>, B.Momo<sup>1</sup>,  
R.B.White<sup>2</sup>, N.Pomphrey<sup>2</sup>, D.A.Spong<sup>3</sup>

<sup>1</sup>*Consorzio RFX – Associazione Euratom-ENEA – Padova, Italy*

<sup>2</sup>*Princeton Plasma Physics Laboratory – Princeton – NJ, USA*

<sup>3</sup>*Oak Ridge National Laboratory – Oak Ridge – TN, USA*

**Transport in RFP SHAx regimes.** The Reversed Field Pinch (RFP) plasmas can spontaneously access regimes in which a single saturated resistive kink mode dominates the magnetic perturbation spectrum (Quasi Single Helicity state, QSH). For sufficiently large values of the dominant mode, the magnetic island separatrix is expelled and a single helical magnetic axis appears. These states are labeled as SHAx (Single Helical Axis) [1]; they are characterized by a helically symmetric core plasma within electron internal transport barriers (ITBs) [2]. SHAx regimes have been discovered and are actively being studied in the RFX-mod device in Padua (Italy) [3] at high plasma currents ( $I_p \approx 1.2-1.8$  MA). The helicity of the dominant mode is  $m=1$ ,  $n=-7$  in RFX-mod and the value of the toroidal component of the magnetic field ( $b_\phi^{1,-7} \approx 20$  mT) at the edge ( $a=0.459$ m) is up to ten times higher than that of the secondary modes and corresponds to 3-4% of the total field axisymmetric component.

In this work we investigate with a test particle approach the transport in these states: on the one hand we consider the effect of the helical geometry and of the residual magnetic chaos; on the other hand we analyze the modification of volume-averaged transport coefficients due to the helical electric field required to satisfy the ambipolar diffusion constraint.

**Particle orbits in RFX-mod helical geometry.** In the ideal limit of vanishing secondary modes the plasma is defined to be in the Single Helicity (SH) regime. The corresponding magnetic topology is reconstructed both by a perturbative approach (by codes such as ORBIT

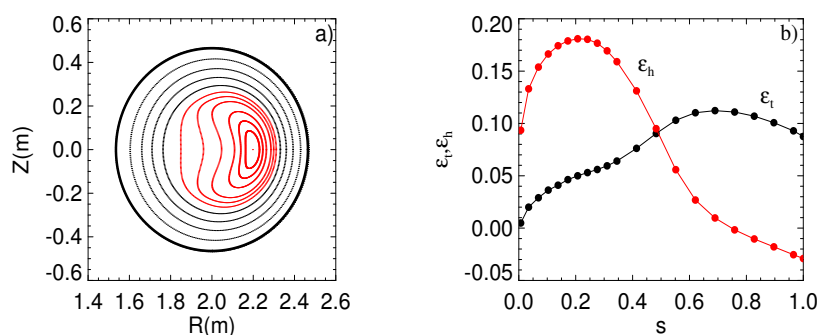


**Figure 1** (a) Reconstruction on a toroidal section of the magnetic topology of a SHAx state in RFX-mod for the RFP-adapted version of the code VMEC. (b) Toroidal (black) and helical (red) ripple versus the normalized poloidal flux for a SHAx state.

[4] or FLiT [5]) and by the VMEC code [6], recently adapted to the RFP configuration.

Fig.1-(a) shows an example of a helical equilibrium calculated by VMEC for RFX-mod. The flux  $s$  enclosed by each of the

helical surfaces can be numerically computed, for example by the method described in [7] by ORBIT, or directly obtained as VMEC output, and used as label for the particle radial position in transport simulations.

The deformation from axisymmetry of the inner magnetic surfaces can be quantified by means of the radial functions  $\varepsilon_h(s)$  and  $\varepsilon_t(s)$ , the helical and the toroidal ripple respectively [8]. They have been determined for RFX-mod from the VMEC output harmonic components: at every magnetic surface the  $n=0$  amplitudes are summed up to estimate  $\varepsilon_t$  while the harmonics with  $n=7$ , the main non-axisymmetric component, are used to evaluate  $\varepsilon_h$ . The radial dependence of these profiles are shown in Fig.1-(b):  $\varepsilon_h$  is dominant in the central region ( $\varepsilon_h \approx 2-3 \varepsilon_t$ ) and close to zero at the edge ( $\varepsilon_h \approx 0.1-0.2 \varepsilon_t$ ). Thus, while the core is strongly helically deformed, the outer region almost preserves the typical properties of a quasi axisymmetric configuration. This particular geometry of helical RFX-mod plasmas has a direct implication in terms of neoclassical transport. In fact, in regions where a significant value of  $\varepsilon_h$  is present, particles with low parallel velocity may become helically trapped (*superbananas*), thus representing a significant source of losses because of their non-zero bounce averaged radial drift [8].

The contribution of superbananas to transport has been investigated by the ORBIT code. We have analyzed the trajectory of an ensemble of collisionless monoenergetic ( $E=0.8keV$ ) trapped particles (ions with pitch  $\lambda = v_{\parallel}/|\mathbf{v}| \sim 0$ , where  $v_{\parallel}$  is the velocity component parallel to the magnetic field  $\mathbf{B}$ ) initially deposited near the helical axis in SH regime in order to quantify the drift effects only due to the helical geometry. The final distribution of the ion pitch absolute values is shown in Fig. 2-(a): the distribution is peaked at  $\lambda \sim 0$  but a tail at higher pitches ( $\lambda > 0.4$ ) typical of passing particles, appears. Fig 2-(b) shows that the small group of

high pitch particles are located in the middle region of the plasma ( $r/a \sim 0.6$ ). In this region the  $\varepsilon_h$  function is rapidly decreasing and therefore trapped particles become passing; as a

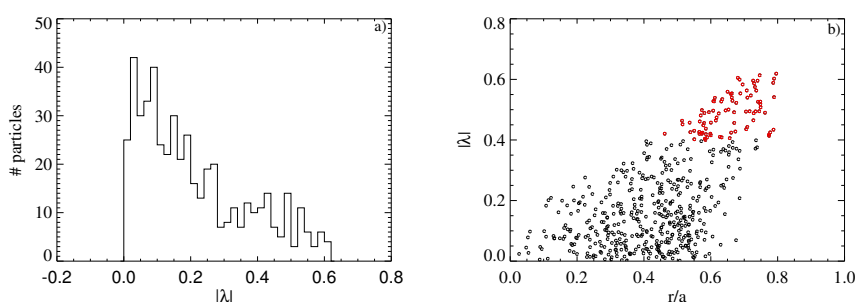


**Figure 2** (a). Pitch absolute values distribution after a simulation by ORBIT. While at the beginning the pitch of all particles is close to zero, a tail at higher values appears by the end. (b) Final pitch versus final radial ion position. In red are the points corresponding to almost passing ions.

consequence they remain confined for a long time without being lost and keeping the same radial position.

The addition of collisions does not substantially change this picture. The effect of collisions on the transport coefficients is reported in Fig. 3-(a) (black line; the collision frequency  $\nu_{\text{coll}}$  is here normalized to the inverse of on axis toroidal transit time  $\tau_{\text{tor}}$ ). Numerical simulations have been performed as described in [7] by calculating the volume-averaged ion diffusion coefficient  $D_i$  in the helical core (domain with red-colored surfaces in Fig.1-(a)) for a group of monoenergetic ions with  $T_e=T_i=0.8\text{keV}$ .  $D_i$  is an increasing function of  $\nu_{\text{coll}} \tau_{\text{tor}}$ : at lower collisionality the  $1/\nu$  regime typical of superbanana orbits is not visible.

**Effect of secondary modes** Even though secondary modes are low, their effect on transport may be significant as they generate a residual level of magnetic chaos. In order to estimate this quantitatively, the algorithm described in [7] has been extended to SHAx states. Results are reported in Fig.3-(a) (red line):  $D_i$  slightly increases in SHAx regimes but with a significant increment only at very low collisionality where  $D_{i,SH} \sim 0.1 D_{i,SHAx}$ .

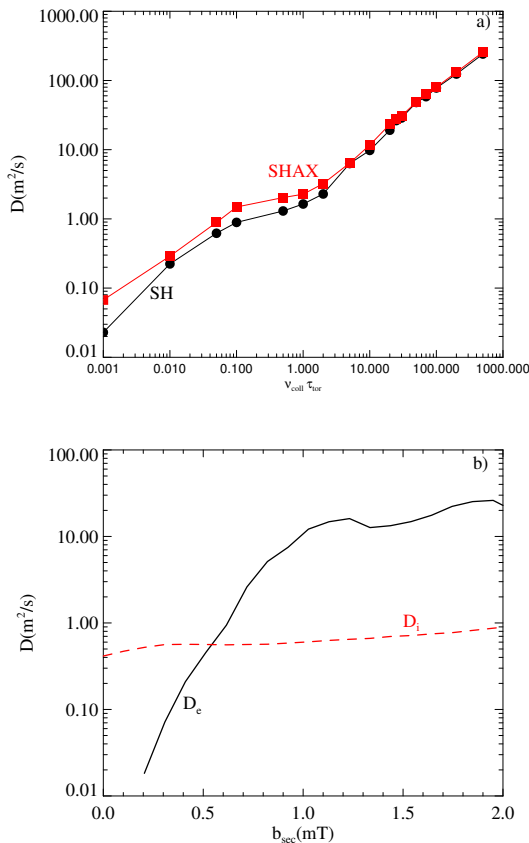


**Figure 3** (a) Ion diffusion coefficients versus collisions for toroidal transit in SH (black) and SHAx (red) states by ORBIT (b) Ion (red) and electron (black) diffusion coefficients as function of the secondary modes amplitude.

In the simulations performed up to now, only ions have been considered. Similar analysis for electrons show that their diffusion coefficient in a pure SH state is ten times smaller than for ions, while in SHAx regimes  $D_e$  strongly depends on the quadratic sum of the amplitude of the secondary mode toroidal components  $b_{\phi,n}$  at the edge:  $b_{\text{sec}} = \sqrt{\sum_{n=8,24} b_{\phi,n}^2(a)}$ .

In the plot of Fig.3-(b) a scan of  $D_i$  and  $D_e$  for a SHAx case is reported; it has been obtained by increasing  $b_{\text{sec}}$  at fixed collisionality, thermal energy and dominant mode amplitude. For the conditions simulated here,  $D_i$  and  $D_e$  are comparable ( $D_i \sim D_e \sim 0.5 \text{m}^2/\text{s}$ ) when  $b_{\text{sec}} \sim 0.4 \text{mT}$ . Since the experimental value is  $b_{\text{sec}} \sim 0.7 \text{mT}$ , corresponding to  $D_e > D_i$ , a radial electric field  $E_r$  must arise in order to ensure ambipolarity.

**Ambipolar radial electric** A simplified model for  $E_r$  has been implemented in the ORBIT code

with the aim to evaluate its effects on ions and electrons transport. As preliminary case, an electrostatic potential  $\Phi$ , constant on each magnetic surface but increasing from the helical axis to the edge, has been considered: thus, the corresponding  $E_r$

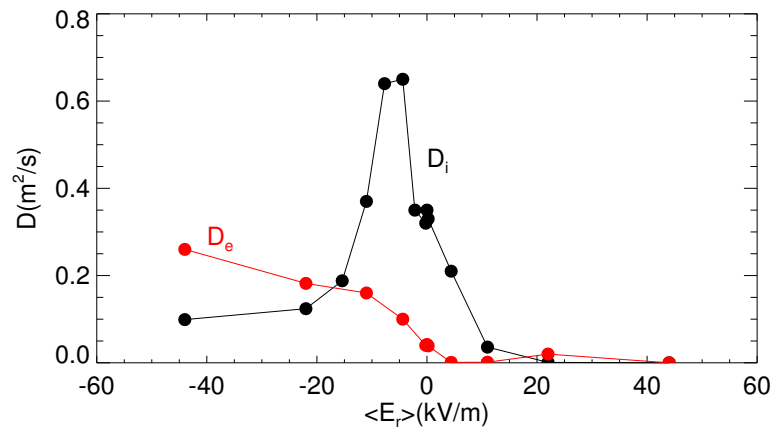


**Figure 4** Ion (black line) and electron (red) diffusion coefficients as function of the average radial electric field near the helical structure O-Point. No secondary modes are included in the simulations.

generated is mainly perpendicular to the helical flux surfaces and the particle orbits in the central region are subjected to a poloidal velocity drift, since the magnetic field is here almost toroidal. Transport simulations have been performed for ions and electrons in a region close to the helical axis (extending radially for 10cm) in a pure SH configuration. The diffusion coefficients have been estimated for different values of  $E_r$  and the results are shown in Fig. 4 where two roots are visible with  $D_e = D_i$ . It is worth to recall that the numerical simulations are performed for mono-energetic particles and experimental temperature and density profiles are not included for the moment. More detailed analysis will take into account these elements too. As next step the condition of ambipolarity will be investigated in the region of the internal transport barrier where  $E_r$  could play an important stabilizing role.

Let us finally note that the availability of the VMEC equilibria is allowing us to estimate neoclassical coefficients with the DKES code [9], which is currently being adapted and used for RFP devices.

**Acknowledgment.** *This work was supported by the European Communities under the contract of Association between EURATOM/ENEA. The views and the opinions expressed herein do not necessarily reflect those of the European Commission.*

#### References

- [1] Lorenzini et al., Nature Physics **5** 570-574 (2009)
- [2] M.E.Puiatti et al., Plasma Phys. Control. Fusion **51** 124031 (2009)
- [3] P. Sonato *et al.*, Fusion Engineering and Design **66**,161 (2003)
- [4] R.B.White and M.S.Chance, Phys. Fluids **27**, 2455 (1984)
- [5] P. Innocente et al., Nucl. Fusion **47**, 1092 (2007)
- [6] Hirshman et al. Phys. Fluids **26** (12) (1983)
- [7] M.Gobbin et al., Phys. Plasmas **14**, 072305 (2007)
- [8] Mynick, Phys. Plasmas **13** 058102 (2006)
- [9] Hirshman et al., Phys. Fluids **29** 2951 (1986)